Achieving High Performance Molecular Rectification through Fast Screening Alkanethiol Carboxylate-Metal Complexes Electro-Active Unites

Lixian Tian[§], Aiqing Fan[§], Xi Yu and Wenping Hu**

Tianjin Key Laboratory of Molecular Optoelectronic Science, School of Science, Tianjin University & Collaborative Innovation Center of Chemical Science and Engineering, Tianjin 300072, China

* Corresponding author E-mail: xi.yu@tju.edu.cn (Xi Yu)

ABSTRACT Achieving high rectifying performance of molecular scale diode devices through synthetic chemistry and device construction remain a formidable challenge due to the complexity of the charge transport process and the device structure. We demonstrated here high-performance molecular rectification realized in self-assembled monolayer (SAM) based device by low-cost and fast screening the electroactive units. SAMs of commercial available carboxylate terminated alkane thiols on gold substrate, coordinated with a variety of metal ions, structures denoting as Au-S-$(CH_2)_{n-1}$COO-M^{m+} (C*n*+M^{m+}), where *n*=11, 12, 13, 14, 16, 18 and M^{m+}=Ca^{2+}, Mn^{2+}, Fe^{2+}, Fe^{3+}, Co^{2+}, Ni^{2+}, Cu^{2+}, Zn^{2+}, were prepared and junctions were measured using a eutectic indium-gallium alloy top contact (EGaIn). The C18+Ca^{2+} and C18+Zn^{2+} junctions were found to afford a record high rectification ratio (RR) of 756 at ±1.5 V. Theoretical analysis based on single level tunneling model shows that optimized combination of the asymmetry voltage division, energy barrier and the coupling of carboxylate-metal complex with electrode. Our method described here represent a general strategy for fast, cheap and effective exploration of the metal complex chemical space for high-performance molecular diodes devices.

TOC GRAPHICS

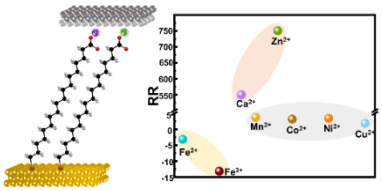

KEYWORDS Molecular diode, EGaIn, self-assembled monolayer, screening

The purpose of molecular electronics is to construct circuits using single or molecular assemblies, and to prepare functional molecular electronic devices with electrical properties determined by the chemical and supramolecular properties of molecules.[1-9] In the past few decades, a verity of functional molecular devices have been theoretically designed and experimentally prepared, such as molecular switches,[10-23] molecular wires,[24-26] negative differential resistance,[27-29] molecular transistors,[30, 31]sensors,[32-34] and molecular diodes.[35-39] The diode is the device that conduct electricity under a forward bias and block under a reverse bias, and is one of the fundamental elements in the circuit. Since Aviram and Ratner first proposed the concept of a molecular diode composed of donor-bridge-acceptor (D-bridge-A) molecules in 1974,[40] many molecular diodes devices have been studied.[38, 41-48]

Since 2010s, molecular diodes based on asymmetric single electronic state[39, 49-51] (Figure 1a) emerged and were extensively developed, mainly by Nijhuis and Whitesides et al,[52, 53] of which significantly, higher rectification ratio (RR) was achieved. This type of molecular rectifier usually utilizes redox active moieties, such like ferrocene,[49, 50, 53, 54] bipyridyl,[39, 55] or various polycyclic-aromatic-hydrocarbon[56] and so on, as active electronic states and inert alkane as spacers for asymmetry. Theoretical study using either ab initio calculation based on DFT and Green's function,[57, 58] or single level transmission models have revealed the origin of the rectification device.[59-61] In the simplified single level model, the current I across the junction is given by the Landauer-Büttiker formula,[62] namely,

$$I = \frac{2e}{h} \int dE[f_L(E) - f_R(E)]\, Tr(E) \qquad (1)$$

where e is the electron charge and h is the Planck's constant. f_L and f_R are the Fermi functions of the left and right electrodes, respectively, given by eq 2.

$$f_{L,R}(E,V) = \frac{1}{\exp\left(\frac{E-eV-\mu_{L,R}}{k_B T}\right)+1} \quad (2)$$

where, $\mu_{L,R}$ is the chemical potential of the left and right electrode. $Tr(E)$ is the transmission function which is related to the coupling strength Γ_L, Γ_R, the energy barrier ε and the voltage division factor or asymmetric factors α, of the single electronic state in the junction, as shown in following eq 3.

$$Tr(E,V,\Gamma_L,\Gamma_R) = \frac{\Gamma_L\Gamma_R}{(E-\varepsilon-\alpha eV)^2+\left[\frac{\Gamma(\Gamma_L,\Gamma_R)}{2}\right]^2} \quad (3)$$

It can be recognized from this model that the rectification is realized when the transmission peak enters the bias window under one bias over the other polarity due to the asymmetricity in the transmission function, as shown in Figure 1b.

In our recent model study, we have extensively studied the performance of the molecular rectifier depending on the coupling strength Γ, energy barrier ε and asymmetric factors α (Figure 1), and the performance optimization of the molecular diode need delicate control on all the three parameters.[60, 61] The theoretical studies imply that, in principle, there exist a big space for rectification performance modulation defined by chemical and device structures. Added on top is the fact that the interface between top electrode, mostly the GaIn/GaO_x, and the molecule is ill-defined due to the unknow composition and structure of GaO_x,[61, 63-65] which further blurred the designing path. Therefore, the performance optimization of the molecular diode through try-and-error strategy by synthetic chemistry and device construction is inevitably a highly time consuming and resource-intensive process.

In the past decade, by various head group and its position and orientation defined by the linker and device structure, the rectification performance based on single state has increased from several tens to 10^3,[49, 50, 66-70] and even reached 10^5,[53] comparable to the practical inorganic p-n junction molecular diodes. However, there still remains a large chemical space to be explored for cheap, reliable and high performance molecular rectification.

In this work, by adopting the idea of in-situ metal ion complex in the SAM,[71, 72] we developed a fast-screening strategy to efficiently explore the junction structure space to achieve high performance molecular rectification. The off-the-shelf carboxylic acid terminated *n*-mercaptoalkanoic acid (*n*=11, 12, 13, 14, 16, 18) SAMs coordinated with various metal ion (M^{m+}=Ca^{2+}, Mn^{2+}, Fe^{2+}, Fe^{3+}, Co^{2+}, Ni^{2+}, Cu^{2+}, Zn^{2+}) were prepared and molecular junction were formed using EGaIn top electrode. Using this fast-screening strategy, Ca^{2+} and Zn^{2+} were filtered out as good electroactive groups for rectification device, of which the RR can reach record high up to ~756 at ±1.5 V by further combing with C18 linker.

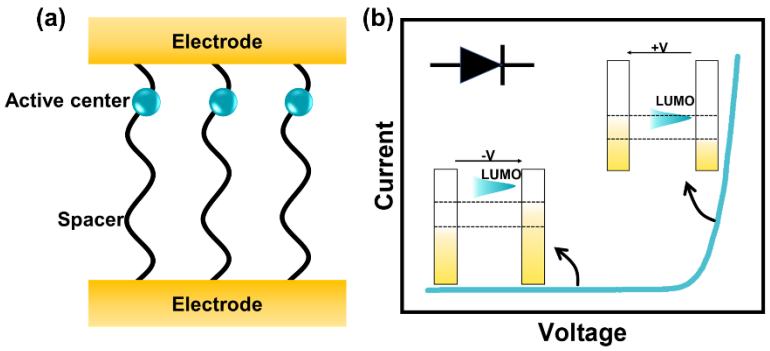

Figure 1. Schematic diagram of the asymmetric molecular junction (left) and I-V characteristic based on the single-level model (right). The horizontal yellow curve represents the shift of LUMO energy level at negative and positive bias. At positive bias, the LUMO energy level

enters the bias window, and the current increases rapidly. While LUMO energy level is outside the bias window at negative bias, and the current is low.

We first prepared and characterized 11-mercaptoundecanoic acid (C11) SAM on the vacuum deposited gold surface, and various metal ions were then coordinated to the SAM surface (C11+M^{m+}; M^{m+}=Ca^{2+}, Mn^{2+}, Fe^{2+}, Fe^{3+}, Co^{2+}, Ni^{2+}, Cu^{2+}, Zn^{2+}). Ellipsometry measurement found an increased thickness of the SAM after metal ion binding (Figure S1a). Surface reflective infrared spectroscopy showed the appearance of carboxylate vibration peak (Figure S1b) and the absence of counter ion Cl^- in complexed SAM (Figure S4a), indicating the formation of the metal ion carboxylate complex, see Supporting Information for details. X-ray photoelectron spectroscopy (XPS) further confirmed the formation of metal complex at the SAM surface with O:M ratio of 4:1, except for Ca^{2+} and Zn^{2+} (2:1), see Table S2.

We further construct the molecular junction (Figure 2) by applying EGaIn on top of the C11+M^{m+} SAM as the top electrode. EGaIn has been well recognized as a stable and harmless soft contact for SAM,[73-75] it is convenient to fabricate and operate, and afford quick and reproducible high yield working junctions, allowing statistically significant data to be collected.[73, 76-79] Our recent work shows that carboxylate alkali metal complexes are beneficial to increase RR, compared with COOH terminated SAM due to the carboxylic acid (COOH)-GaO_x/GaIn interface.[61]

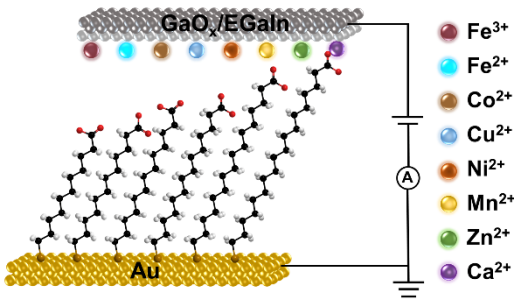

Figure 2. Schematic illustration of the molecular junction based on metal-organic coordinated monolayer of Au-C*n*+M^{m+}-GaO_x/EGaIn, where *n*=11, 12, 13, 14, 16, 18, M^{m+}=Ca^{2+}, Mn^{2+}, Fe^{2+}, Fe^{3+}, Co^{2+}, Ni^{2+}, Cu^{2+}, Zn^{2+}.

The C11+M^{m+} SAM junctions of 8 types were measured and the I-V response and rectification performance was summarized in Figure 3. We define the rectification ratio RR as the current density *J* ratio at positive and negative bias voltages (RR=|*J*(+V)|/|*J*(−V)| at ±1.5 V or ±1 V), and the value and positive/negative sign indicate the magnitude and polarity of the rectification.

The averaged Log *J*-V traces of the C11-COOH and C11+M^{m+} junctions are shown in Figure 3a, Figure S5. Figure S4 in supporting information provides statistical heat map of *J*-V plots. It can be seen that various C11+M^{m+} exhibited quite different rectification behavior. Cu^{2+}, Mn^{2+}, Co^{2+}, and Ni^{2+} junctions have very low positive RR (<5), while Fe^{2+} and Fe^{3+} exhibit lightly negative RR (-2 and -13) respectively. In contrast, Zn^{2+} and Ca^{2+} junction afford much higher positive RR (more than 40).

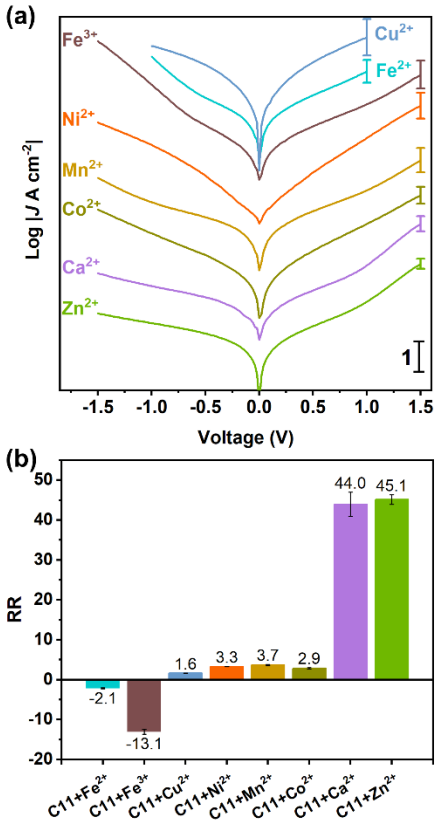

Figure 3. Transport behavior and rectification performance of the 11-mercaptoalkanoate-metal complexes monolayer junction ($C11+M^{m+}$) junctions. (a) The averaged Log |*J*|-V traces of the $C11+M^{m+}$ junctions. The *J*-V traces were shifted vertically for a clearer view, while keeping the same scale. The vertical bar represents 1 order of magnitude. (b) Rectification ratio (RR=|*J*(+1.5 V)|/|*J*(−1.5 V)|) of the junctions. RR of Cu^{2+} and Fe^{2+} was calculated at 1.0 V because they were easy to get shorts above +1.0 V.

The rectification direction of Ca^{2+} and Zn^{2+} complexed SAM junction along with all the $C11+M^{m+}$ junctions of positive RR is the same as COOH terminated SAM junction,[61, 80] while opposite to that of the Fc-based junction,[68, 81] implying the electronic state of energy higher than the Fermi level of the electrode, which is often LUMO, dominates the charge transport process and should be responsible for the rectification for all the junctions with positive RR. When a

positive bias is applied, the energy level of the metal ion atomic orbital enters the bias window, causing the current to increase rapidly, thereby causing rectification (Figure 1b). On the contrary, electronic state of energy lower than the Fermi level of the electrode, which is often HOMO, should dominates the charge transport process in Fe^{2+}, Fe^{3+} junction, and is responsible for the negative RR.

As we have discussed before, RR of the single state-based rectification device is jointly affected by several physical parameters like the voltage division factor (α), the coupling (Γ) and the energy offset (ε) of the electronic state with respect to the electrode. Considering the voltage division factor is mainly determined by the spatial position of the electronic state in the junction, we can assume that α is the same for all the C11+M^{m+} junction. Then the high performance of Ca^{2+} and Zn^{2+} may be due to the appropriate energy offset and coupling with top electrode GaO_x/GaIn.

We next try to further increase the performance of the molecular diode by introducing more asymmetry on voltage division factor. This was done by applying longer linker between bottom electrode and carboxylate metal, i.e. we constructed SAM of C*n*+Ca^{2+}/Zn^{2+} where *n*=11, 12, 13, 14, 16, 18). SAM thickness, and structures were extensively characterized as well by ellipsometry, IRRAS, and XPS (Figure S8-S10). Figure 4 showed the *J*-V traces and rectification performance of the C*n*+Ca^{2+}/Zn^{2+} junctions (Figure S11 provides the heat maps of all the *J*-V traces). We can find the off-state current density *J* at negative bias decreases gradually as the chain length increases, while keep almost constant at positive bias, which leads to an increase of RR (Figure 4a,b). Meanwhile, it can also be found that there is a sharp increase of *J* value at on-state voltage around 1 V (arrow in Figure 4a,b), which can be recognized as the sign that the available electronic state enters the bias window. While at the negative bias (-1.5 V) range, the

electronic state is always outside the bias window. At the same time, the RR^{+} increases as the voltage increases (Figure 4c, d). We summarized the RR of C*n*+Ca^{2+}/Zn^{2+} at ±1.5 V as shown in Figure 5. As the number of carbon atoms *n* increases from 11 to 18, the RR increases from 45 to 573 and 756 for Ca^{2+} and Zn^{2+}, respectively.

We also studied the effect of the linker on other metal ions carboxylate complex (shown in Figure S16, S17a) and observed a similar, but smaller increase in RR in the C18 complex except for Fe^{2+}, Fe^{3+} and Cu^{2+}, the RR increased from 4 to 19, 3.2 to 131, 3.5 to 28 for Mn^{2+}, Co^{2+} and Ni^{2+} respectively (Figure S17b).

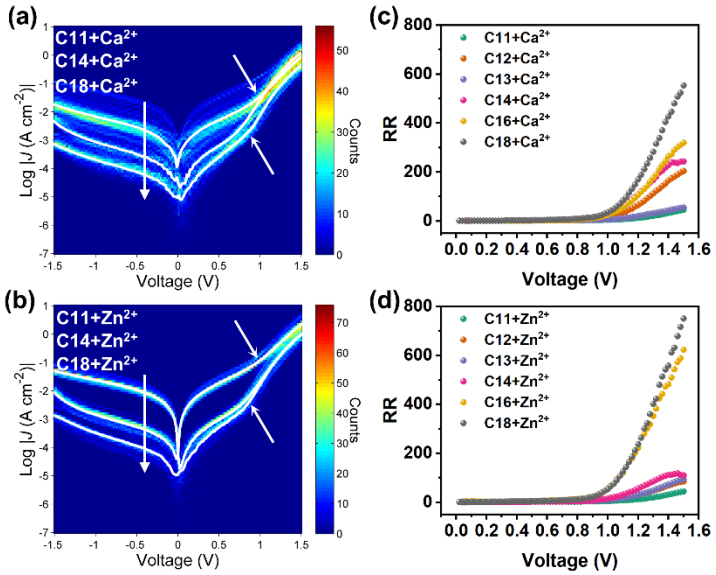

Figure 4. Heat maps and average Log |*J*|-V curves (white) (a, b) and RR(V) (c, d) for *n*-mercaptoalkanoate-Ca^{2+}/Zn^{2+} complexes monolayer junction (C*n*+Ca^{2+}/Zn^{2+}, *n*=11, 12, 13, 14, 16, 18).

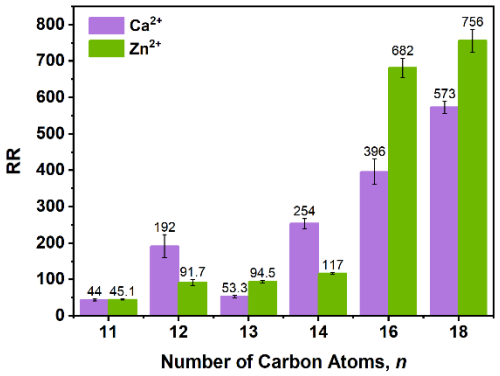

Figure 5. RR at ±1.5 V of *n*-mercaptoalkanoate-Ca^{2+}/Zn^{2+} complexes monolayer junction (C*n*+Ca^{2+}/Zn^{2+}, *n*=11, 12, 13, 14, 16, 18). The error bars represent one standard deviation.

We try to further model the performance of the C*n*+Ca^{2+}/Zn^{2+} using the single level tunneling model.[61, 82] As described above, the improvement of RR depends on the energy barrier ε, coupling strength Γ and the asymmetry factor α.[50, 69, 83-88] In our model, we set the energy barrier ε value to 1.0 eV. We assume that the coupling strength between carboxylate metal complex and the Au substrate decreases exponentially with the number of carbon atoms following $\Gamma_B = Ae^{-\beta L_B}$,[60] where A is contact coupling constant. β is the attenuation coefficient. L_B is the number of carbon atoms of active group from the bottom electrode. And α decreases linearly with the increase of the number of carbon atoms following $\alpha = B - DL_B$, where B is asymmetry factor at zero spacer length and D is the rate with length. For detailed analysis of these values, please see the Supporting Information.

The simulated change of Log *I*-V curves versus chain lengths is shown in Figure 6. We can see that the current decreases significantly with the alkyl chain length at negative bias while the positive bias current at high voltage decrease little, leading to increased, which agree well with the experimental results. Moreover, we can also find the threshold voltage at which current increases sharply, i.e. the resonance threshold, is decreased with increasing chain length, as

shown in red arrow of Figure 6. This is due to the increased asymmetry of the junction, which can bring the resonance peak into the bias window at lower voltage. The same trend can also be found in the experimental study as shown in Figure 4.

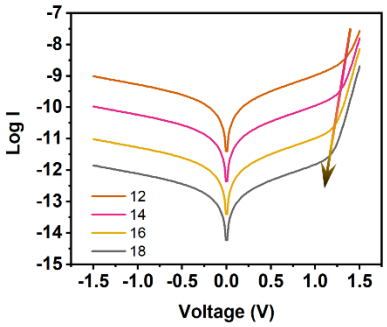

Figure 6. Simulated Log *I*-V curves of different chain lengths by single level tunneling model. The energy barrier is 1.0 eV, and the coupling strength decrease exponentially with the number of carbon atoms. The asymmetry factor decreases linearly with the number of carbon atoms. The arrow is the indicator that the threshold voltage decreases as the number of carbon atoms increases.

Table 1. Summary of RR Larger 50 Based on Monolayer Molecular Junctions Using EGaIn as Top Electrode

bottom electrode	SAM structure	voltage (V)	RR	refs
Au^{TS}	HSC_9Fc	1.0	1.7(-)	86
Au^{TS}	$HSC_{11}Fc$	1.0	3.1(-)	86
Au^{TS}	$HSC_{13}Fc$	1.0	1.7(-)	86
Ag^{TS}	HSC_9Fc	1.0	120(-)	67, 86
Ag^{TS}	$HSC_{11}Fc$	1.0	~100(-)	52, 54, 67, 68, 81, 86, 89-91
Ag^{TS}	$HSC_{13}Fc$	1.0	81(-)	50, 86

Ag^{TS}	$HSC_{10}NHC{=}OFc$	1.0	90(-)	[54]
Ag^{TS}	$HSC_{11}FcC_2$	1.0	77.43(-)	50
Ag^{TS}	$HSC_{11}Fc_2$	1.0	500(-)	[52, 81, 90]
Ag^{TS}	$HSC_{11}Fc{=}Fc^{\alpha}$	0.875	1100(-)	49
Ag^{TS}	$HSC_{11}Fc\text{-}Fc$	1.125	610(-)	49
Ag^{TS}	$HSC_{15}Fc\text{-}C{\equiv}C\text{-}Fc$	1.0	1000(-)	[53]
Ag^{TS}	$HSC_{15}Fc\text{-}C{\equiv}C\text{-}Fc$	2.0	794 (-)	[53]
Pt^{TS}	$HSC_{15}Fc\text{-}C{\equiv}C\text{-}Fc$	1.0	398(-)	[53]
Pt^{TS}	$HSC_{15}Fc\text{-}C{\equiv}C\text{-}Fc$	3.0	6×10^5(-)	[53]
Au^{TS}	$HSC_{15}Fc\text{-}C{\equiv}C\text{-}Fc$	1.0	251(-)	[53]
Au^{TS}	$HSC_{15}Fc\text{-}C{\equiv}C\text{-}Fc$	3.0	1×10^4 (-)	[53]
Ag^{TS}	$HSC_{11}BIPY$	1.0	85(+)	39
Au^{TS}	$HSC_{11}BIPY$	1.0	40(+)	39
Au^{TS}	$HSC_{11}BIPY\text{-}MCl_2$ (M=Mn, Fe, Co)	1.0	~80(+)	[71]
Au^{TS}	HSC_{11}S-BTTF Benzotetrathiafulvalene (BTTF)	1.5	83(+)	[66]
Pt^{TS}	HSC_{11}S-BTTF Benzotetrathiafulvalene BTTF	2.5	912(-)	[66]
Ag^{TS}	HSC_{11} PAH polycyclic-aromatic-hydrocarbon (PAH)	0.74 1.0	~170(-) ~150(-)	[56]

[a] $RR^+=|J(+V)|/|J(-V)|$ and $RR^-=|J(-V)|/|J(+V)|$; ^{TS}: Abbreviation for template stripping.

In summary, we demonstrated in this work a quick screening strategy to efficiently explore the chemical space for high performance molecular rectification based on carboxylate-metal complexes electro-active unites. By studying a series of junctions with the structure of Au-S-C_n-

$_1COO^-M^{m+}$//GaO_x/EGaIn, where n=11, 12, 13, 14, 16, 18; M^{m+}=Ca^{2+}, Mn^{2+}, Fe^{2+}, Fe^{3+}, Co^{2+}, Ni^{2+}, Cu^{2+}, Zn^{2+}, we have reached RR as high 750 at ±1.5 V using Ca^{2+} and Zn^{2+} combined with C18-COOH SAM. Table 1 summarizes the RR larger than 50 in single level molecular junction fabricated with the EGaIn top electrode, and the C18+Zn^{2+} junction in this work is among one of the best molecular diodes, while it is much easier and cheaper to make than other type of molecular diodes.

We would like to emphasize that there still remain a large metal complex space of different metal ions and ligands to be explored using our strategy. And it is worth noting as well that the rectification obtained in this work is based on a relative rough gold surface (Rq=0.7 nm), so a higher performance diode is expected to be realized on template stripped ultra-flat substrate.

ASSOCIATED CONTENT

Supporting Information.

The Supporting Information is available free of charge.
Experimental section; characterization of n-mercaptoalkanoate-M^{m+} SAMs; coordination structure of carboxylic acid metal complex; and single level tunneling model (PDF)

AUTHOR INFORMATION

Corresponding Author

Xi Yu − Tianjin Key Laboratory of Molecular Optoelectronic Science, School of Science, Tianjin University & Collaborative Innovation Center of Chemical Science and Engineering, Tianjin 300072, China; ID orcid.org/0000-0001-5750-7003; Email: xi.yu@tju.edu.cn

Wenping Hu − Tianjin Key Laboratory of Molecular Optoelectronic Science, School of Science, Tianjin University & Collaborative Innovation Center of Chemical Science and Engineering, Tianjin 300072, China; Joint School of National University of Singapore and Tianjin University, Fuzhou 350207, China; ID orcid.org/0000-0001-5686-2740; Email: huwp@tju.edu.cn

Authors

Lixian Tian − Tianjin Key Laboratory of Molecular Optoelectronic Science, School of Science, Tianjin University & Collaborative Innovation Center of Chemical Science and Engineering, Tianjin 300072, China

Aiqing Fan − Tianjin Key Laboratory of Molecular Optoelectronic Science, School of Science, Tianjin University & Collaborative Innovation Center of Chemical Science and Engineering, Tianjin 300072, China

Author Contributions

[§]L. T. and A. F. contributed equally to this work.

Notes

The authors declare no competing financial interests.

ACKNOWLEDGMENT

This work was supported by the National Natural Science Foundation of China (21973069, 21773169), the National Key R&D Program (2017YFA0204503 and 2016YFB0401100), the PEIYANG Young Scholars Program of Tianjin University (2018XRX-0007), the Industry-

University-Research Cooperation Program of Tianjin University and Qinghai Nationalities University (2021XZC-0064).

REFERENCES

(1) Xiang, D.; Wang, X.; Jia, C.; Lee, T.; Guo, X. Molecular-Scale Electronics: From Concept to Function. *Chem. Rev.* **2016**, *116*, 4318-4440.

(2) Li, J.; Wu, Q.; Xu, W.; Wang, H.-C.; Zhang, H.; Chen, Y.; Tang, Y.; Hou, S.; Lambert, C. J.; Hong, W. Room-Temperature Single-Molecule Conductance Switch via Confined Coordination-Induced Spin-State Manipulation. *CCS Chem.* **2021**, 1744-1752.

(3) McCreery, R. L.; Bergren, A. J. Progress with Molecular Electronic Junctions: Meeting Experimental Challenges in Design and Fabrication. *Adv. Mater.* **2009**, *21*, 4303-4322.

(4) Lin, S.; Lai, W. K.; Li, Y.; Lu, W.; Bai, G.; Lau, S. P. Liquid-Phase Exfoliation of Violet Phosphorus for Electronic Applications. *SmartMat.* **2021**, *2*, 226-233.

(5) Aradhya, S. V.; Venkataraman, L. Single-Molecule Junctions beyond Electronic Transport. *Nat. Nanotechnol.* **2013**, *8*, 399-410.

(6) Jeong, H.; Kim, D.; Xiang, D.; Lee, T. High-Yield Functional Molecular Electronic Devices. *ACS Nano* **2017**, *11*, 6511-6548.

(7) Geng, Y.; Zhao, Y.; Zhao, J.; Zhai, Y.; Yuan, M.; Wang, X.-D.; Gao, H.; Feng, J.; Wu, Y.; Jiang, L. Optical and Electrical Modulation in Ultraviolet Photodetectors Based on Organic One-Dimensional Photochromic Arrays. *SmartMat.* **2021**, *2*, 388-397.

(8) Liu, Y.; Qiu, X.; Soni, S.; Chiechi, R. C. Charge Transport through Molecular Ensembles: Recent Progress in Molecular Electronics. *Chem. Phys. Rev.* **2021**, *2*, 021303.

(9) Wang, S.; Liu, S.; Sulkanen, A.; Fox, J. M.; Jia, X.; Liu, G.-y. Controlled Molecular Assembly of Tetrazine Derivatives on Surfaces. *CCS Chem.* **2021**, 1789-1799.

(10) Jan van der Molen, S.; Liljeroth, P. Charge Transport through Molecular Switches. *J. Phys.: Condens. Matter* **2010**, *22*, 133001.

(11) Donhauser, Z. J.; Mantooth, B. A.; Kelly, K. F.; Bumm, L. A.; Monnell, J. D.; Stapleton, J. J.; Price, D. W., Jr.; Rawlett, A. M.; Allara, D. L.; Tour, J. M., et al. Conductance Switching in Single Molecules through Conformational Changes. *Science* **2001**, *292*, 2303-2307.

(12) Zhang, J. L.; Zhong, J. Q.; Lin, J. D.; Hu, W. P.; Wu, K.; Xu, G. Q.; Wee, A. T.; Chen, W. Towards Single Molecule Switches. *Chem. Soc. Rev.* **2015**, *44*, 2998-3022.

(13) Su, T. A.; Li, H.; Steigerwald, M. L.; Venkataraman, L.; Nuckolls, C. Stereoelectronic Switching in Single-Molecule Junctions. *Nat. Chem.* **2015**, *7*, 215-220.

(14) Roldan, D.; Kaliginedi, V.; Cobo, S.; Kolivoska, V.; Bucher, C.; Hong, W.; Royal, G.; Wandlowski, T. Charge Transport in Photoswitchable Dimethyldihydropyrene-Type Single-Molecule Junctions. *J. Am. Chem. Soc.* **2013**, *135*, 5974-5977.

(15) Jia, C.; Migliore, A.; Xin, N.; Huang, S.; Wang, J.; Yang, Q.; Wang, S.; Chen, H.; Wang, D.; Feng, B., et al. Covalently Bonded Single-Molecule Junctions with Stable and Reversible Photoswitched Conductivity. *Science* **2016**, *352*, 1443-1445.

(16) Thompson, D.; Barco, E. d.; Nijhuis, C. A. Design Principles of Dual-Functional Molecular Switches in Solid-State Tunnel Junctions. *Appl. Phys. Lett.* **2020**, *117*, 030502.

(17) Tang, C.; Zheng, J.; Ye, Y.; Liu, J.; Chen, L.; Yan, Z.; Chen, Z.; Chen, L.; Huang, X.; Bai, J., et al. Electric-Field-Induced Connectivity Switching in Single-Molecule Junctions. *iScience* **2020**, *23*, 100770.

(18) Qiu, X.; Ivasyshyn, V.; Qiu, L.; Enache, M.; Dong, J.; Rousseva, S.; Portale, G.; Stohr, M.; Hummelen, J. C.; Chiechi, R. C. Thiol-Free Self-Assembled Oligoethylene Glycols Enable Robust Air-Stable Molecular Electronics. *Nat. Mater.* **2020**, *19*, 330-337.

(19) Huang, X.; Li, T. Recent Progress in the Development of Molecular-Scale Electronics Based on Photoswitchable Molecules. *J. Mater. Chem. C* **2020**, *8*, 821-848.

(20) Hnid, I.; Frath, D.; Lafolet, F.; Sun, X.; Lacroix, J. C. Highly Efficient Photoswitch in Diarylethene-Based Molecular Junctions. *J. Am. Chem. Soc.* **2020**, *142*, 7732-7736.

(21) Atesci, H.; Kaliginedi, V.; Celis Gil, J. A.; Ozawa, H.; Thijssen, J. M.; Broekmann, P.; Haga, M. A.; van der Molen, S. J. Humidity-Controlled Rectification Switching in Ruthenium-Complex Molecular Junctions. *Nat. Nanotechnol.* **2018**, *13*, 117-121.

(22) Audi, H.; Viero, Y.; Alwhaibi, N.; Chen, Z.; Iazykov, M.; Heynderickx, A.; Xiao, F.; Guérin, D.; Krzeminski, C.; Grace, I. M., et al. Electrical Molecular Switch Addressed by Chemical Stimuli. *Nanoscale* **2020**, *12*, 10127-10139.

(23) Kumar, S.; Merelli, M.; Danowski, W.; Rudolf, P.; Feringa, B. L.; Chiechi, R. C. Chemical Locking in Molecular Tunneling Junctions Enables Nonvolatile Memory with Large On-Off Ratios. *Adv. Mater.* **2019**, *31*, 1807831.

(24) Kuang, G.; Chen, S. Z.; Wang, W.; Lin, T.; Chen, K.; Shang, X.; Liu, P. N.; Lin, N. Resonant Charge Transport in Conjugated Molecular Wires beyond 10 nm Range. *J. Am. Chem. Soc.* **2016**, *138*, 11140-11143.

(25) Leary, E.; Limburg, B.; Alanazy, A.; Sangtarash, S.; Grace, I.; Swada, K.; Esdaile, L. J.; Noori, M.; Gonzalez, M. T.; Rubio-Bollinger, G., et al. Bias-Driven Conductance Increase with Length in Porphyrin Tapes. *J. Am. Chem. Soc.* **2018**, *140*, 12877-12883.

(26) Wardrip, A. G.; Mazaheripour, A.; Husken, N.; Jocson, J. M.; Bartlett, A.; Lopez, R. C.; Frey, N.; Markegard, C. B.; Kladnik, G.; Cossaro, A., et al. Length-Independent Charge Transport in Chimeric Molecular Wires. *Angew. Chem. Int. Ed. Engl.* **2016**, *55*, 14267-14271.

(27) Tivanski, A. V.; Walker, G. C. Ferrocenylundecanethiol Self-Assembled Monolayer Charging Correlates with Negative Differential Resistance Measured by Conducting Probe Atomic Force Microscopy. *J. Am. Chem. Soc.* **2005**, *127*, 7647-7653.

(28) He, J.; Lindsay, S. M. On the Mechanism of Negative Differential Resistance in Ferrocenylundecanethiol Self-Assembled Monolayers. *J. Am. Chem. Soc.* **2005**, *127*, 11932-11933.

(29) Chen, J.; Reed, M. A.; Rawlett, A. M.; Tour, J. M. Large On-Off Ratios and Negative Differential Resistance in a Molecular Electronic Device. *Science* **1999**, *286*, 1550-1552.

(30) Song, H.; Kim, Y.; Jang, Y. H.; Jeong, H.; Reed, M. A.; Lee, T. Observation of Molecular Orbital Gating. *Nature* **2009**, *462*, 1039-1043.

(31) Pan, Y.; Wang, Y.; Wang, L.; Zhong, H.; Quhe, R.; Ni, Z.; Ye, M.; Mei, W. N.; Shi, J.; Guo, W., et al. Graphdiyne-Metal Contacts and Graphdiyne Transistors. *Nanoscale* **2015**, *7*, 2116-2127.

(32) Schedin, F.; Geim, A. K.; Morozov, S. V.; Hill, E. W.; Blake, P.; Katsnelson, M. I.; Novoselov, K. S. Detection of Individual Gas Molecules Adsorbed on Graphene. *Nat. Mater.* **2007**, *6*, 652-655.

(33) Adjizian, J.-J.; Leghrib, R.; Koos, A. A.; Suarez-Martinez, I.; Crossley, A.; Wagner, P.; Grobert, N.; Llobet, E.; Ewels, C. P. Boron- and Nitrogen-Doped Multi-Wall Carbon Nanotubes for Gas Detection. *Carbon* **2014**, *66*, 662-673.

(34) Xie, Z.; Zuo, X.; Zhang, G.-P.; Li, Z.-L.; Wang, C.-K. Detecting CO, NO and NO_2 Gases by Boron-Doped Graphene Nanoribbon Molecular Devices. *Chem. Phys. Lett.* **2016**, *657*, 18-25.

(35) Chen, X.; Yeganeh, S.; Qin, L.; Li, S.; Xue, C.; Braunschweig, A. B.; Schatz, G. C.; Ratner, M. A.; Mirkin, C. A. Chemical Fabrication of Heterometallic Nanogaps for Molecular Transport Junctions. *Nano Lett.* **2009**, *9*, 3974-3979.

(36) Capozzi, B.; Xia, J.; Adak, O.; Dell, E. J.; Liu, Z. F.; Taylor, J. C.; Neaton, J. B.; Campos, L. M.; Venkataraman, L. Single-Molecule Diodes with High Rectification Ratios through Environmental Control. *Nat. Nanotechnol.* **2015**, *10*, 522-527.

(37) Metzger, R. M. Unimolecular Electrical Rectifiers. *Chem. Rev.* **2003**, *103*, 3803-3834.

(38) Diez-Perez, I.; Hihath, J.; Lee, Y.; Yu, L.; Adamska, L.; Kozhushner, M. A.; Oleynik, I. I.; Tao, N. Rectification and Stability of a Single Molecular Diode with Controlled Orientation. *Nat. Chem.* **2009**, *1*, 635-641.

(39) Yoon, H. J.; Liao, K. C.; Lockett, M. R.; Kwok, S. W.; Baghbanzadeh, M.; Whitesides, G. M. Rectification in Tunneling Junctions: 2,2'-Bipyridyl-Terminated n-Alkanethiolates. *J. Am. Chem. Soc.* **2014**, *136*, 17155-17162.

(40) Aviram, A.; Ratner, M. A. Molecular Rectifiers. *Chem. Phys. Lett.* **1974**, *29*, 277-283.

(41) Metzger, R. M. Unimolecular Rectifiers: Present Status. *Chem. Phys.* **2006**, *326*, 176-187.

(42) Metzger, R. M. Unimolecular Electronics. *Chem. Rev.* **2015**, *115*, 5056-5115.

(43) Johnson, M. S.; Kota, R.; Mattern, D. L.; Metzger, R. M. Janus Reversal and Coulomb Blockade in Ferrocene-Perylenebisimide and N,N,N',N'-Tetramethyl-*para*-phenylenediamine-Perylenebisimide D-σ-A Rectifiers. *Langmuir* **2016**, *32*, 6851-6859.

(44) Metzger, R. M.; Chen, B.; Höpfner, U.; Lakshmikantham, M. V.; Vuillaume, D.; Kawai, T.; Wu, X.; Tachibana, H.; Hughes, T. V.; Sakurai, H., et al. Unimolecular Electrical Rectification in Hexadecylquinolinium Tricyanoquinodimethanide. *J. Am. Chem. Soc.* **1997**, *119*, 10455-10466.

(45) Wang, B.; Zhou, Y.; Ding, X.; Wang, K.; Wang, X.; Yang, J.; Hou, J. G. Conduction Mechanism of Aviram-Ratner Rectifiers with Single Pyridine-σ-C_{60} Oligomers. *J. Phys. Chem. B* **2006**, *110*, 24505-24512.

(46) Morales, G. M.; Jiang, P.; Yuan, S.; Lee, Y.; Sanchez, A.; You, W.; Yu, L. Inversion of the Rectifying Effect in Diblock Molecular Diodes by Protonation. *J. Am. Chem. Soc.* **2005**, *127*, 10456-10457.

(47) Hihath, J.; Bruot, C.; Nakamura, H.; Asai, Y.; Diez-Perez, I.; Lee, Y.; Yu, L.; Tao, N. Inelastic Transport and Low-Bias Rectification in a Single-Molecule Diode. *ACS Nano* **2011**, *5*, 8331-8339.

(48) Zhang, G.-P.; Hu, G.-C.; Song, Y.; Li, Z.-L.; Wang, C.-K. Modulation of Rectification in Diblock Co-oligomer Diodes by Adjusting Anchoring Groups for Both Symmetric and Asymmetric Electrodes. *J. Phys. Chem. C* **2012**, *116*, 22009-22014.

(49) Yuan, L.; Breuer, R.; Jiang, L.; Schmittel, M.; Nijhuis, C. A. A Molecular Diode with a Statistically Robust Rectification Ratio of Three Orders of Magnitude. *Nano Lett.* **2015**, *15*, 5506-5512.

(50) Yuan, L.; Nerngchamnong, N.; Cao, L.; Hamoudi, H.; del Barco, E.; Roemer, M.; Sriramula, R. K.; Thompson, D.; Nijhuis, C. A. Controlling the Direction of Rectification in a Molecular Diode. *Nat. Commun.* **2015**, *6*, 6324.

(51) Zhang, G.; Ratner, M. A.; Reuter, M. G. Is Molecular Rectification Caused by Asymmetric Electrode Couplings or by a Molecular Bias Drop? *J. Phys. Chem. C* **2015**, *119*, 6254-6260.

(52) Nijhuis, C. A.; Reus, W. F.; Siegel, A. C.; Whitesides, G. M. A Molecular Half-Wave Rectifier. *J. Am. Chem. Soc.* **2011**, *133*, 15397-15411.

(53) Chen, X.; Roemer, M.; Yuan, L.; Du, W.; Thompson, D.; Del Barco, E.; Nijhuis, C. A. Molecular Diodes with Rectification Ratios Exceeding 10^5 Driven by Electrostatic Interactions. *Nat. Nanotechnol.* **2017**, *12*, 797-803.

(54) Song, P.; Yuan, L.; Roemer, M.; Jiang, L.; Nijhuis, C. A. Supramolecular vs Electronic Structure: The Effect of the Tilt Angle of the Active Group in the Performance of a Molecular Diode. *J. Am. Chem. Soc.* **2016**, *138*, 5769-5772.

(55) Kang, H.; Kong, G. D.; Byeon, S. E.; Yang, S.; Kim, J. W.; Yoon, H. J. Interplay of Fermi Level Pinning, Marcus Inverted Transport, and Orbital Gating in Molecular Tunneling Junctions. *J. Phys. Chem. Lett.* **2020**, *11*, 8597-8603.

(56) Cho, S. J.; Kong, G. D.; Park, S.; Park, J.; Byeon, S. E.; Kim, T.; Yoon, H. J. Molecularly Controlled Stark Effect Induces Significant Rectification in Polycyclic-Aromatic-Hydrocarbon-Terminated *n*-Alkanethiolates. *Nano Lett.* **2019**, *19*, 545-553.

(57) Zhang, G.-P.; Chen, L.-Y.; Zhao, J.-M.; Sun, Y.-Z.; Shi, N.-P.; Wang, M.-L.; Hu, G.-C.; Wang, C.-K. Large Rectification Ratio of up to 10^6 for Conjugation-Group-Terminated Undecanethiolate Single-Molecule Diodes on Pt Electrodes. *J. Phys. Chem. C* **2021**, *125*, 20783-20790.

(58) Wei, M.-Z.; Fu, X.-X.; Wang, Z.-Q.; Hu, G.-C.; Li, Z.-L.; Wang, C.-K.; Zhang, G.-P. Bias and Molecular-Length Dependent Odd-Even Effect of Rectification in 4'-Methyl-2,2'-Bipyridyl-Terminated n-Alkanethiolate Single-Molecule Diodes. *J. Mater. Chem. C* **2019**, *7*, 9000-9007.

(59) Garrigues, A. R.; Yuan, L.; Wang, L.; Mucciolo, E. R.; Thompon, D.; Del Barco, E.; Nijhuis, C. A. A Single-Level Tunnel Model to Account for Electrical Transport through Single Molecule- and Self-Assembled Monolayer-based Junctions. *Sci. Rep.* **2016**, *6*, 26517.

(60) Song, X.; Yu, X.; Hu, W. Model Study on the Ideal Current-Voltage Characteristics and Rectification Performance of a Molecular Rectifier under Single-Level-Based Tunneling and Hopping Transport. *J. Phys. Chem. C* **2020**, *124*, 24408-24419.

(61) Tian, L.; Song, X.; Yu, X.; Hu, W. Modulated Rectification of Carboxylate-Terminated Self-Assembled Monolayer Junction by Humidity and Alkali Metal Ions: The Coupling and Asymmetric Factor Matter. *J. Phys. Chem. C* **2021**, *125*, 21614-21623.

(62) Datta, S. *Quantum Transport: Atom to Transistor*; Cambridge University Press: Cambridge, 2005.

(63) Carlotti, M.; Degen, M.; Zhang, Y.; Chiechi, R. C. Pronounced Environmental Effects on Injection Currents in EGaIn Tunneling Junctions Comprising Self-Assembled Monolayers. *J. Phys. Chem. C* **2016**, *120*, 20437-20445.

(64) Martin, A.; Du, C.; Chang, B.; Thuo, M. Complexity and Opportunities in Liquid Metal Surface Oxides. *Chem. Mater.* **2020**, *32*, 9045-9055.

(65) Cutinho, J.; Chang, B. S.; Oyola-Reynoso, S.; Chen, J.; Akhter, S. S.; Tevis, I. D.; Bello, N. J.; Martin, A.; Foster, M. C.; Thuo, M. M. Autonomous Thermal-Oxidative Composition Inversion and Texture Tuning of Liquid Metal Surfaces. *ACS Nano* **2018**, *12*, 4744-4753.

(66) Han, Y.; Maglione, M. S.; Diez Cabanes, V.; Casado-Montenegro, J.; Yu, X.; Karuppannan, S. K.; Zhang, Z.; Crivillers, N.; Mas-Torrent, M.; Rovira, C., et al. Reversal of the Direction of Rectification Induced by Fermi Level Pinning at Molecule-Electrode Interfaces in Redox-Active Tunneling Junctions. *ACS Appl. Mater. Interfaces* **2020**, *12*, 55044-55055.

(67) Nerngchamnong, N.; Yuan, L.; Qi, D. C.; Li, J.; Thompson, D.; Nijhuis, C. A. The Role of Van Der Waals Forces in the Performance of Molecular Diodes. *Nat. Nanotechnol.* **2013**, *8*, 113-118.

(68) Nijhuis, C. A.; Reus, W. F.; Whitesides, G. M. Molecular Rectification in Metal-SAM-Metal Oxide-Metal Junctions. *J. Am. Chem. Soc.* **2009**, *131*, 17814-17827.

(69) Thompson, D.; Nijhuis, C. A. Even the Odd Numbers Help: Failure Modes of SAM-Based Tunnel Junctions Probed via Odd-Even Effects Revealed in Synchrotrons and Supercomputers. *Acc. Chem. Res.* **2016**, *49*, 2061-2069.

(70) Nijhuis, C. A.; Reus, W. F.; Barber, J. R.; Dickey, M. D.; Whitesides, G. M. Charge Transport and Rectification in Arrays of SAM-Based Tunneling Junctions. *Nano Lett.* **2010**, *10*, 3611-3619.

(71) Park, J.; Belding, L.; Yuan, L.; Mousavi, M. P. S.; Root, S. E.; Yoon, H. J.; Whitesides, G. M. Rectification in Molecular Tunneling Junctions Based on Alkanethiolates with Bipyridine-Metal Complexes. *J. Am. Chem. Soc.* **2021**, *143*, 2156-2163.

(72) Li, Y.; Root, S. E.; Belding, L.; Park, J.; Rawson, J.; Yoon, H. J.; Baghbanzadeh, M.; Rothemund, P.; Whitesides, G. M. Characterizing Chelation at Surfaces by Charge Tunneling. *J. Am. Chem. Soc.* **2021**, *143*, 5967-5977.

(73) Chiechi, R. C.; Weiss, E. A.; Dickey, M. D.; Whitesides, G. M. Eutectic Gallium-Indium (EGaIn): A Moldable Liquid Metal for Electrical Characterization of Self-Assembled Monolayers. *Angew. Chem. Int. Ed. Engl.* **2008**, *47*, 142-144.

(74) Dickey, M. D.; Chiechi, R. C.; Larsen, R. J.; Weiss, E. A.; Weitz, D. A.; Whitesides, G. M. Eutectic Gallium-Indium (EGaIn): A Liquid Metal Alloy for the Formation of Stable Structures in Microchannels at Room Temperature. *Adv. Funct. Mater.* **2008**, *18*, 1097-1104.

(75) Cademartiri, L.; Thuo, M. M.; Nijhuis, C. A.; Reus, W. F.; Tricard, S.; Barber, J. R.; Sodhi, R. N. S.; Brodersen, P.; Kim, C.; Chiechi, R. C., et al. Electrical Resistance of Ag^{TS}–$S(CH_2)_{n-1}CH_3$//Ga_2O_3/EGaIn Tunneling Junctions. *J. Phys. Chem. C* **2012**, *116*, 10848-10860.

(76) Kumar, S.; van Herpt, J. T.; Gengler, R. Y.; Feringa, B. L.; Rudolf, P.; Chiechi, R. C. Mixed Monolayers of Spiropyrans Maximize Tunneling Conductance Switching by Photoisomerization at the Molecule-Electrode Interface in EGaIn Junctions. *J. Am. Chem. Soc.* **2016**, *138*, 12519-12526.

(77) Yoon, H. J.; Bowers, C. M.; Baghbanzadeh, M.; Whitesides, G. M. The Rate of Charge Tunneling Is Insensitive to Polar Terminal Groups in Self-Assembled Monolayers in $Ag^{TS}S(CH_2)_nM(CH_2)_mT//Ga_2O_3$/EGaIn Junctions. *J. Am. Chem. Soc.* **2014**, *136*, 16-19.

(78) Simeone, F. C.; Yoon, H. J.; Thuo, M. M.; Barber, J. R.; Smith, B.; Whitesides, G. M. Defining the Value of Injection Current and Effective Electrical Contact Area for EGaIn-Based Molecular Tunneling Junctions. *J. Am. Chem. Soc.* **2013**, *135*, 18131-18144.

(79) Nijhuis, C. A.; Reus, W. F.; Barber, J. R.; Whitesides, G. M. Comparison of SAM-Based Junctions with Ga_2O_3/EGaIn Top Electrodes to Other Large-Area Tunneling Junctions. *J. Phys. Chem. C* **2012**, *116*, 14139-14150.

(80) Ai, Y.; Kovalchuk, A.; Qiu, X.; Zhang, Y.; Kumar, S.; Wang, X.; Kuhnel, M.; Norgaard, K.; Chiechi, R. C. In-Place Modulation of Rectification in Tunneling Junctions Comprising Self-Assembled Monolayers. *Nano Lett.* **2018**, *18*, 7552-7559.

(81) Nijhuis, C. A.; Reus, W. F.; Whitesides, G. M. Mechanism of Rectification in Tunneling Junctions Based on Molecules with Asymmetric Potential Drops. *J. Am. Chem. Soc.* **2010**, *132*, 18386-18401.

(82) Tian, L.; Martine, E.; Yu, X.; Hu, W. Amine-Anchored Aromatic Self-Assembled Monolayer Junction: Structure and Electric Transport Properties. *Langmuir* **2021**, *37*, 12223-12233.

(83) Kornilovitch, P. E.; Bratkovsky, A. M.; Stanley Williams, R. Current Rectification by Molecules with Asymmetric Tunneling Barriers. *Phys. Rev. B* **2002**, *66*, 165436.

(84) Liu, R.; Ke, S. H.; Yang, W.; Baranger, H. U. Organometallic Molecular Rectification. *J. Chem. Phys.* **2006**, *124*, 024718.

(85) Milan, D. C.; Vezzoli, A.; Planje, I. J.; Low, P. J. Metal Bis(Acetylide) Complex Molecular Wires: Concepts and Design Strategies. *Dalton Trans.* **2018**, *47*, 14125-14138.

(86) Yuan, L.; Thompson, D.; Cao, L.; Nerngchangnong, N.; Nijhuis, C. A. One Carbon Matters: The Origin and Reversal of Odd–Even Effects in Molecular Diodes with Self-Assembled Monolayers of Ferrocenyl-Alkanethiolates. *J. Phys. Chem. C* **2015**, *119*, 17910-17919.

(87) Moth-Poulsen, K.; Bjornholm, T. Molecular Electronics with Single Molecules in Solid-State Devices. *Nat. Nanotechnol.* **2009**, *4*, 551-556.

(88) Taylor, J.; Brandbyge, M.; Stokbro, K. Theory of Rectification in Tour Wires: The Role of Electrode Coupling. *Phys. Rev. Lett.* **2002**, *89*, 138301.

(89) Yuan, L.; Jiang, L.; Thompson, D.; Nijhuis, C. A. On the Remarkable Role of Surface Topography of the Bottom Electrodes in Blocking Leakage Currents in Molecular Diodes. *J. Am. Chem. Soc.* **2014**, *136*, 6554-6557.

(90) Reus, W. F.; Thuo, M. M.; Shapiro, N. D.; Nijhuis, C. A.; Whitesides, G. M. The SAM, Not the Electrodes, Dominates Charge Transport in Metal-Monolayer//Ga_2O_3/Gallium-Indium Eutectic Junctions. *ACS Nano* **2012**, *6*, 4806-4822.

(91) Jiang, L.; Yuan, L.; Cao, L.; Nijhuis, C. A. Controlling Leakage Currents: The Role of the Binding Group and Purity of the Precursors for Self-Assembled Monolayers in the Performance of Molecular Diodes. *J. Am. Chem. Soc.* **2014**, *136*, 1982-1991.